

Author Manuscript

Title: Anisotropic conductivity at the single molecule scale

Authors: Sepideh Afsari Mamaghani; Parisa Yasini; Haowei Peng; John P. Perdew;
Eric Borguet

This is the author manuscript accepted for publication and has undergone full peer review but has not been through the copyediting, typesetting, pagination and proofreading process, which may lead to differences between this version and the Version of Record.

To be cited as: 10.1002/anie.201903898

Link to VoR: <https://doi.org/10.1002/anie.201903898>

Anisotropic conductivity at the single molecule scale

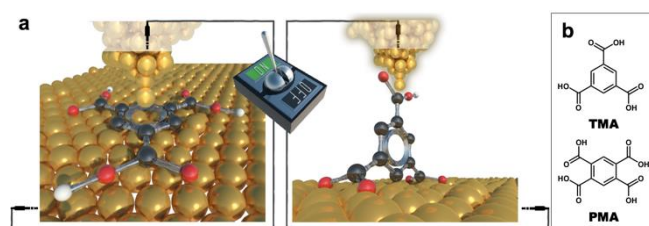
Sepideh Afsari,^[a] Parisa Yasini,^[a] Haowei Peng,^[b] John P. Perdew,^{[a],[b]} and Eric Borguet*^[a]

Abstract: In most junctions built by wiring a single molecule between two electrodes, the electrons flow along only one axis: between the two anchoring groups. However, molecules can be anisotropic and an orientation-dependent conductance is expected. Here, we fabricate single molecule junctions using the electrode potential to control the molecular orientation and access individual elements of the conductivity tensor. We measure the conductance in two directions; along the molecular plane as the benzene ring bridges two electrodes using anchoring groups (upright); and orthogonal to the molecular plane with the molecule lying flat on the substrate (planar). The perpendicular (planar) conductance is ~ 400 x higher than along the molecular plane (upright). This offers a new method for designing a reversible single molecule electromechanical switch that at room-temperature controllably employs the electrode potential to orient the molecule in the junction between “ON” and “OFF” conductance states.

Introduction

The ultimate goal in the development of nano-electronics is controllable charge transport through molecules that operate as electronic components^[1] such as rectifiers^[2] and switches.^[3] In studying molecular conductance at the single molecule level, junctions are typically fabricated by wiring a single molecule between two metal electrodes via anchoring groups^[4,5] such as thiols^[6] and amines^[7] that provide sufficient electronic coupling between the metal and the molecule. The contact between the single molecule and the electrodes must be robust, reproducible and able to provide a strong contact between the molecule and the electrodes so that the junction is stable and has a low contact resistance.^[8] In such conventional single molecule conductivity (SMC) measurements, charge transport is measured along one axis, i.e., between two anchoring groups.^[8,9] Our previous study in measuring charge transport perpendicular to the aromatic ring of a benzene derivative for the first time, revealed that junctions formed via direct contact between the gold electrodes and the π system of benzene results in a molecular conductance that is two orders of magnitude higher than the conductance of a benzene ring connected via standard anchoring groups.^[10] Furthermore, DFT calculations showed that the conductance perpendicular to the

^[11] ring is about $0.1 G_0$ ^[12–14] ($G_0 = 2e^2/h$ where e is the electron charge and h is Planck's constant^[4]) while the conductance of single benzene derivative junctions formed with standard linker groups is about 0.005 – $0.01 G_0$.^[15]



Scheme 1. (a) Schematic of two possible junction configurations formed by direct interaction of the Au electrodes to either the aromatic ring or the carboxylic acid groups of single TMA molecules. (b) Molecular structure of the benzene carboxylic acids used in this study.

These observations led us to the hypothesis that for any benzene derivative, there could be an orientation-dependent conductance in the junction. Thus, the conductance of single molecule junctions is anisotropic, due to the different possible contact geometries, i.e. electrode-anchoring groups (upright/vertical) versus direct electrode- π contact (planar/horizontal), and likely associated with very different conductance values. Since any structural transformation of single-molecule junctions triggered by an external chemical or physical stimulus (i.e. applied force,^[16] light,^[17] tunneling current,^[18] redox reaction^[11,19] or change in pH^[20]) that results in altered electronic properties of the molecular junction can be utilized in designing single molecule electronic switches,^[21] we propose employing this strategy to design an electromechanical single molecule switch. We show that we can controllably alternate our single molecule switch between high or “ON” and low or “OFF” conductance modes by employing an external stimulus that induces a transition in the single molecule orientation in the junction from “planar” to “upright” (Scheme 1a).

Results and Discussion

Two benzenecarboxylic acids including trimesic acid (TMA) and pyromellitic acid (PMA) containing three and four peripheral carboxylic groups (COOH) respectively (Scheme 1b) are used in this study to build molecular junctions. We reproducibly fabricate orientation-controlled single molecule junctions utilizing a combination of electrochemical scanning tunneling microscopy (EC-STM) break junction (EC-STM-BJ) and high resolution STM imaging under electrode potential control (for details see Experimental Section). The potential of the gold electrode surface (working electrode) is employed to control the orientation of the single molecule in the junction between the gold tip and electrode

[a] Dr. Sepideh Afsari, Parisa Yasini, Dr. Eric Borguet
Department of Chemistry
Temple University
1901 N. 13th St., Philadelphia, PA 19122
E-mail: eborguet@temple.edu

[b] Dr. Haowei Peng, Dr. John P. Perdew
Department of Physics
Temple University
1925 N 12th St., Philadelphia, PA 19122

Supporting information for this article is given via a link at the end of the document.

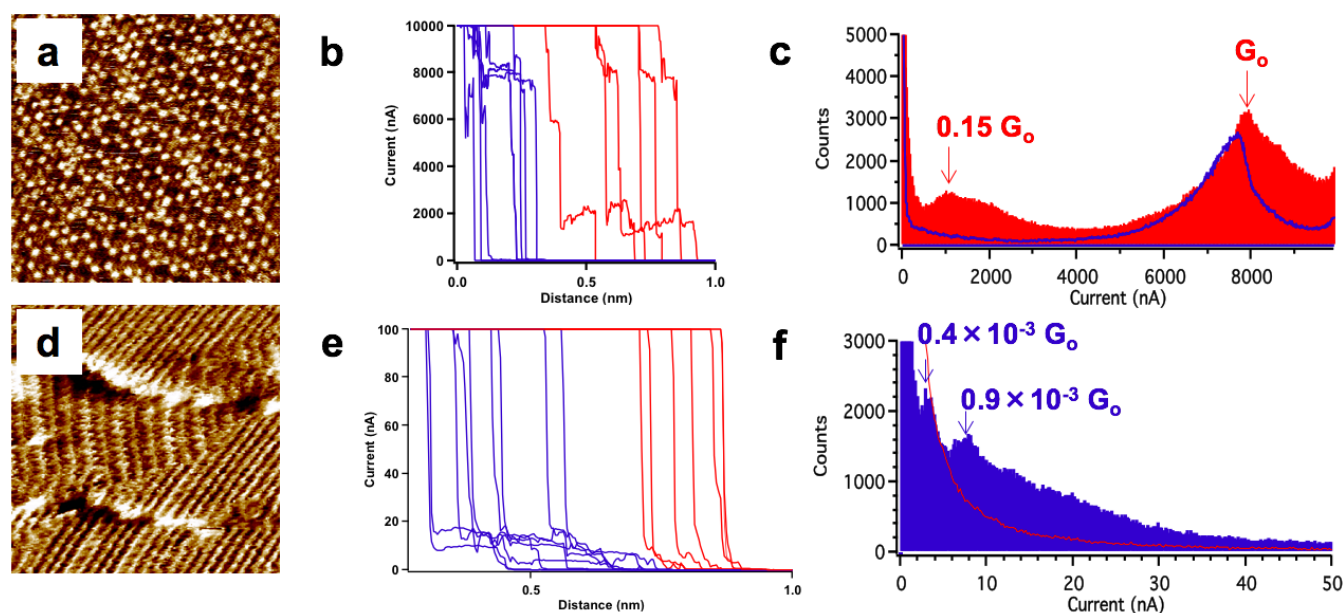


Figure 1. STM imaging and conductance measurements of trimesic acid (TMA) (a) 20x20 nm² EC-STM image of TMA on a negatively charged ($E_{\text{surface}} = -0.10 \text{ V}_{\text{SCE}}$) Au(111) electrode indicating benzene rings parallel to the surface. (b) Example of individual current-distance traces at high current regions collected on negatively (red) and positively (blue) charged Au(111) surfaces. (c) All-data point EC-STM-BJ current histograms of TMA at high current regions collected on a negatively charged ($E_{\text{surface}} = -0.10 \text{ V}_{\text{SCE}}$) Au(111) electrode without any data selection of 9070 individual current-distance traces (red) and on a positively charged ($E_{\text{surface}} = +0.75 \text{ V}_{\text{SCE}}$) Au(111) electrode without any data selection of 7609 individual current-distance traces (blue). (d) 10x10 nm² EC-STM image of TMA on a positively charged Au(111) electrode ($E_{\text{surface}} = +0.75 \text{ V}_{\text{SCE}}$) Au(111) electrode showing an ordered structure of TMA molecules standing upright. (e) Example of individual current-distance traces collected on negatively (red) and positively (blue) charged Au(111) surfaces. (f) All-data point EC-STM-BJ current histograms of TMA at low current regions collected on a positively charged Au(111) electrode ($E_{\text{surface}} = +0.75 \text{ V}_{\text{SCE}}$) without any data selection of 2974 individual current-distance traces (blue) and a negatively charged Au(111) electrode ($E_{\text{surface}} = -0.10 \text{ V}_{\text{SCE}}$) without any data selection of 2970 individual current-distance traces (red).

surface while the conductivity of the single molecule is measured for each orientation. The anisotropic conductivity of single-molecule junctions in two orientations (upright and planar) of the central benzene rings (Scheme 1a) is investigated. TMA molecules (Scheme 1b) are adsorbed in planar geometry at negatively charged Au surface with the benzene ring oriented parallel to the surface.^[22] We show that junctions formed with planar orientation have a conductance about one-tenth of the conductance quantum, G_0 . This conductance is significantly higher than that achieved with an upright orientation of TMA molecules in the junction and also more than two orders of magnitude higher than the conductance of single molecule junctions of benzene derivatives formed with conventional linkers such as thiols and amines.^[15] The high conductance we observe suggests strongly that direct coupling between the π system of the benzene ring and the gold STM tip results in charge transport perpendicular to the benzene ring. This hypothesis is well supported by density functional theory (DFT) calculations in this study for TMA, with the calculated conductance about 300 times higher for the planar than the upright orientation. Hence, the electrode potential can, in principle, be employed as an external stimulus to switch orientation of a single molecule in an electrical junction inducing on or off conductance states of a single molecule switch.

As the first step in fabricating the proposed electromechanical single molecule switch, we conducted EC-STM imaging to clarify

the molecule orientation on the charged Au surface. The potential of zero charge, where the surface charge is zero, for the electrochemically reconstructed Au(111)-(22x√3) and the Au(111)-(1x1) surfaces are 270 mV and 230 mV versus SCE, respectively.^[23] STM images of the electrified Au(111) electrode show that TMA molecules (Scheme 1b) are physisorbed at negative potentials (or negative surface charge densities) with the benzene ring lying flat on the gold electrode surface forming long range ordered structures due to intermolecular hydrogen bonds between COOH groups (Figure 1a). Moving to positive potentials (positive surface charge densities) TMA molecules are chemisorbed with the ring oriented upright due to deprotonation of COOH groups^[24] and coordinating to the gold electrode (Figure 1d) (STM image analysis can be found in Supporting Information, S2).

Following the STM imaging, SMC measurements were conducted to form planar TMA single-molecule junctions by repeatedly bringing the STM tip into contact with the electrified Au(111) electrode in the presence of the TMA monolayer while current-distance traces were recorded in the 1-10000 nA current range. Displacement of the STM tip away from the negatively charged Au (111) ($E_{\text{surface}} = -0.1 \text{ V}_{\text{SCE}}$) in the presence of the TMA monolayer gave rise to quasi-exponentially decaying traces that are interrupted by current plateau (or steps) interpreted as resulting from molecular junction formation, allowing the current to remain approximately constant even as the distance of the tip-

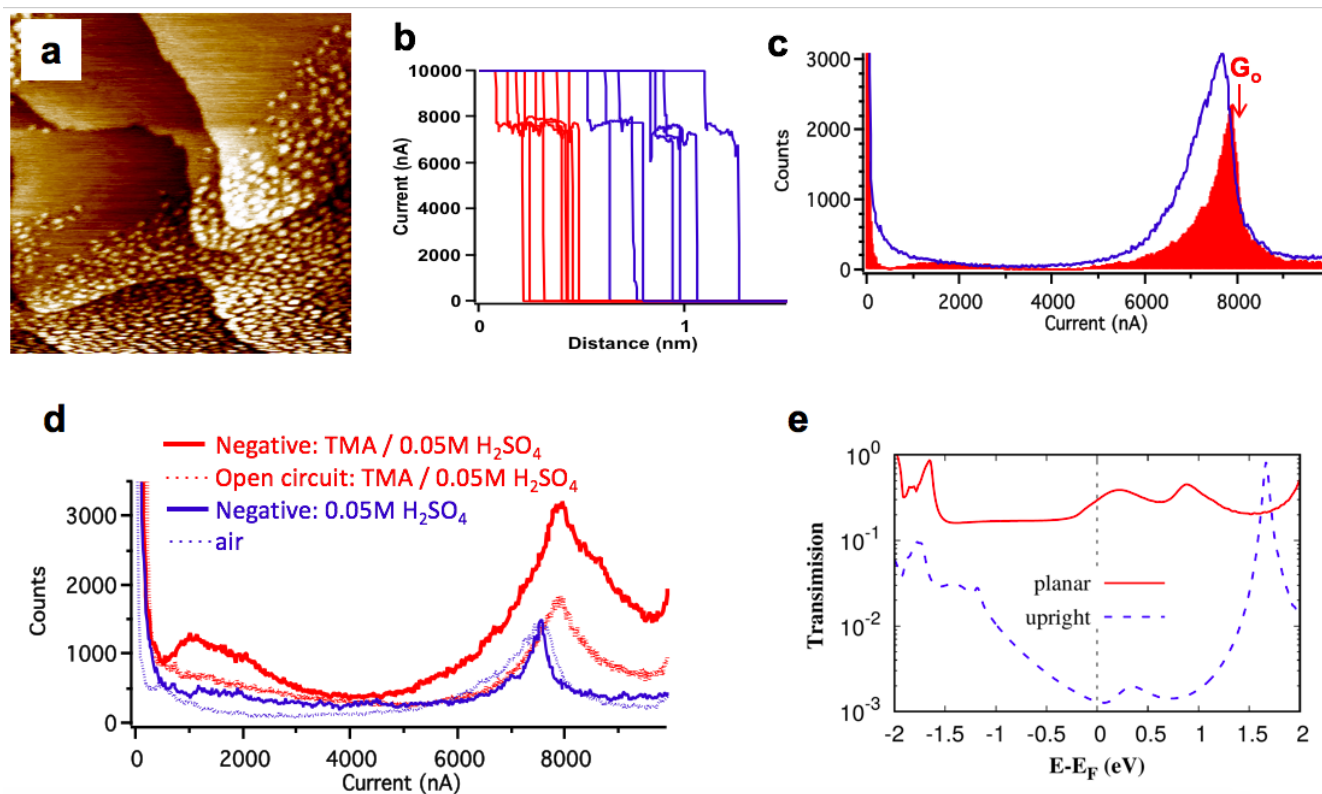


Figure 2. Control STM imaging and conductance measurements and DFT calculations. (a) $100 \times 100 \text{ nm}^2$ EC-STM image of pyromellitic acid (PMA) on a negatively charged ($E_{\text{surface}} = -0.10 \text{ V}_{\text{SCE}}$) Au(111). (b) Example of individual current-distance traces collected in the presence of pyromellitic acid (PMA) on negatively (red) and positively (blue) charged Au(111) electrodes without any data selection of 5029 and 3071 individual current-distance traces, respectively. (c) EC-STM-BJ current histograms of PMA on negatively (red) and positively (blue) charged Au(111) electrodes without any data selection. (d) STM-BJ current histograms without any data selection of (solid red line): TMA in $0.05 \text{ M H}_2\text{SO}_4$ on a negatively charged Au(111) ($E_{\text{surface}} = -0.10 \text{ V}_{\text{SCE}}$ and $E_{\text{bias}} = -0.10 \text{ V}$), (dotted red line): TMA in $0.05 \text{ M H}_2\text{SO}_4$ and no electrode potential control on Au(111) ($E_{\text{bias}} = -0.10 \text{ V}$), (solid blue line): $0.05 \text{ M H}_2\text{SO}_4$ without TMA on a negatively charged Au(111) ($E_{\text{surface}} = -0.10 \text{ V}_{\text{SCE}}$ and $E_{\text{bias}} = -0.10 \text{ V}$), (dotted blue line): Au(111) in air ($E_{\text{bias}} = -0.10 \text{ V}$). (e) The transmission spectra for TMA single molecule junctions between the Au(111) surface and STM tip for both the planar and upright TMA orientation.

substrate increases (Figure 1b, red traces). A statistical assessment of repeated EC-STM-BJ measurements is provided by conductance histograms, generated without any data selection from over 10,000 measurements, that show a clear peak at a conductance value of $0.15 G_0$ for negative potentials (Figure 1c, red). At positive potentials, only quasi-exponentially decaying traces without any plateau or steps are observed suggesting the absence of molecules bridging the electrode potential toward positive values (Figure 1b, blue traces). Thus, the conductance peak observed at $0.15 G_0$ disappears by changing the electrode potential toward positive values (Figure 1c, blue).

As a control, and in order to verify that the observed conductance peak corresponds to single TMA molecules, we measured conductance in the absence of the TMA monolayer (Figure 2d). These histograms are generated without any data selection from over 2000 current-distance measurements on Au(111) in air, in sulfuric acid (without TMA) at negative potentials and 1 mM TMA in sulfuric acid without electrode potential control (Details of SMC experiments can be found in Supporting Information, S1d). In none of these control STM-BJ

measurements, all characterized by the absence of the ordered TMA monolayer, do we see a peak corresponding to the charge transport through molecular junctions (Figure 2d) confirming that the $0.15 G_0$ peak represents the conductance of single molecule junctions formed with TMA molecules in the assembled monolayer. Additionally, to confirm the bias potential dependence, we investigated the current-bias relationship for this conductance feature by varying the bias voltage (E_{bias}) from -0.10 V to -0.05 V in SMC experiments while the $E_{\text{surface}} = -0.1 \text{ V}_{\text{SCE}}$ is maintained negatively charged surface (Supporting Information, S3). The current peak in the histogram (Figure S3B) moves to lower currents proportionally to E_{bias} in accordance with Ohm's law ($V=IR$), and the resulting conductance is constant.

In our STM-BJ measurements, because the maximum current typically only allows the detection of the conductance quantum, G_0 ($\sim 77500 \text{ nA}$ at $E_{\text{bias}} = 100 \text{ mV}$), the contact is insufficient to make more than a single Au atom junction. Therefore, we conclude that neither the tip nor the overall monolayer are destroyed.^[10] We attribute the $0.15 G_0$ conductance peak to charge transport perpendicular to the benzene ring (Scheme 1a).

Intermolecular hydrogen bonding between neighboring molecules immobilizes TMA molecules on the Au(111) surface allowing direct contact between the Au electrodes and the π system of the benzene ring. In these junctions, the benzene ring is planar on the gold substrate thus charge transport between the electrodes is perpendicular to that plane.

Next, we investigated the “off” conductance state of the TMA single molecule switch under positive potentials and in much lower current regions (1-100 nA). Changing the gold electrode potential to positive values drives the molecular orientation from planar to upright (Figure 1d) due to deprotonation of the carboxylic acid groups.^[24] Ordered structures of TMA molecules are formed by pairs of upright and parallel-aligned TMA molecules coordinated to the positively charged substrate surface via one deprotonated carboxylate (COO^-) group and possible formation of intermolecular hydrogen bonds involving the solution-directed carboxyl (COOH) groups.^[25] In this arrangement, the parallel phenyl rings of one dimer are separated by 0.35 nm (Supporting Information, Figure S2 C and D). The single molecule junctions on a positively charged Au(111) surface ($E_{\text{surface}} = +0.75 \text{ V}_{\text{SCE}}$) are expected to be formed with contacts between carboxylic acid groups and gold electrodes (Scheme 1a) leading to a current plateau or step in the current-distance traces (Figure 1e, blue traces) in the low current regions. Thus, the 0.15 G_0 (high) conductance peak disappears and two (low) conductance peaks at about $0.4 \times 10^{-3} \text{ G}_0$ and $0.9 \times 10^{-3} \text{ G}_0$ are present in the histograms (Figure 1f, blue). When measuring the conductance of the single molecules at the junction, it is possible that molecules deviate from the idealized perfectly planar or upright geometries. However, the lengths of the molecular junctions in current-distance traces shown in Figure 1b and 1e are consistent with flat-oriented and upright molecules, respectively. Furthermore, when the molecules deviate from the ideal configurations, charge transport through such geometries should result in the broadening of the conductance peak in the current histogram.

Previously reported conductance values of single molecule junctions formed with 1-4 benzenedithiol range from 0.01 G_0 to $4 \times 10^{-4} \text{ G}_0$.^[15,26-28] This leads us to attribute the $0.4 \times 10^{-3} \text{ G}_0$ peak to the conductance of single TMA molecules bridging the electrodes through the carboxylic acid groups while we suggest that the $0.9 \times 10^{-3} \text{ G}_0$ peak is the collective conductance due to the simultaneous contact between two (pairs of upright and parallel-aligned) TMA molecules and the STM tip. Neither of these conductance peaks was observed in histograms acquired at negative potentials (Figure 1f, red). We believe that hydrogen bonding between neighboring TMA molecules at the negatively charged surface is strong enough to keep the molecules parallel to the surface. Thus, junctions with direct contact between the carboxylic acid groups and the gold electrodes cannot easily be formed at negative potentials, leading to current-distance traces without any current plateau or step in the low current region (Figure 1e, red traces).

In order to confirm that the observed peaks at $0.4 \times 10^{-3} \text{ G}_0$ and $0.9 \times 10^{-3} \text{ G}_0$ actually represent the signature of molecular conductance, we investigated the current-bias relationship for these conductance features by varying the bias voltage (E_{bias}) from -0.10 V to -0.30 V in SMC experiments while the potential of the surface (E_{surface}) is maintained at $+0.75 \text{ V}_{\text{SCE}}$ (Supporting

Information, S4). The current maxima in the histograms increase proportionally to E_{bias} revealing a constant conductance (Figure S4B). The bias independence of the conductance indicates the molecular nature of the conductance peaks attributed to transport through the benzene ring of the upright TMA molecule in the junction with carboxylic acid groups as linkers.

To further test the hypothesis that a planar geometry stabilized by long range ordered structures is necessary to observe the high conductance state, we measured transport through pyromellitic acid (PMA), which by design and due to the hindrance of four carboxylic acid groups (Scheme 1b), appears unlikely to form long range ordered structure with a planar geometry of benzene rings on the gold substrate.^[29] Thus, direct Au- π contact is rarely formed because the molecule is unlikely to be oriented with its benzene ring perpendicular to the junction axis.

Our STM images of PMA do not reveal any ordered structure (Figure 2a). Instead, the surface is covered with bright features varying in size from one to several nm that can be tentatively assigned to clusters of a few PMA molecules agglomerated due to hydrogen bonding between the carboxylic acid groups (Figure 2a). The conductance histograms of PMA collected with negative and positive potentials are similar. Notably, the dominant 0.15 G_0 peak is missing in both histograms (Figure 2c red and blue). Instead, a few broad peaks are present (Figure 2c, red) quite unlike the feature for TMA.

In order to confirm that the peaks we observe in the PMA histogram are not dominant enough to be attributed to a molecular conductance of a specific geometry, we can compare the amplitude of the peaks in the region of 0-2000 nA with the height of G_0 peak. In the TMA histograms collected with the same experimental setup (negatively charged Au(111) surface), the peak in the region of 0-2000 nA is clear with a height about one fourth of the G_0 peak (Figure 1c) while in the PMA histogram, the minor peaks are at most one tenth of the G_0 peak (Figure 2c). We also conducted SMC experiments for PMA in the low current region (1-100 nA) and we did not see any peak corresponding to charge transport through junctions formed via carboxylic linkers (Supporting Information, S5). These control measurements show that in the case of PMA, where no long-range order was observed, single-molecule junctions with the benzene ring perpendicular to the Au STM tip are not formed.

To further elucidate that such an ON/OFF switching does not arise from some uncertainty related to the atomic-level details within our experimental setting, we performed DFT calculations with the SIESTA^[30] and TranSIESTA.^[31] We used the Troullier-Martins norm-conservation pseudopotentials,^[32] the so-called SZP pseudo-atomic orbital (PAO) basis for Au, DZP basis for other elements, and the consistent- exchange van der Waals density functional (vdW-DF-cx)^[33] for the exchange correlation approximation. The computation procedure is available in Supporting Information S6. For the planar orientation, the benzene ring takes the hcp-A configuration,^[34] and for the upright orientation, the deprotonated COOH groups directly bond to Au atoms of the Au(111) substrate as in the experiment. The transmission spectrum from non-equilibrium Green's functional computation is shown in Figure 2e, where the transmission at the Fermi level is an excellent estimator for low-bias conductance. Thanks to some error cancellation, the DFT

results, 0.3 and 0.001 G_0 for the planar and upright orientations respectively, agrees quite well the experimental values. More importantly, the DFT computation confirms that such strong orientation dependence is intrinsic.

Based on these observations and calculations, we conclude that we controllably measured charge transport/conductance along two different axes: one with the benzene ring lying flat on the substrate perpendicular to the STM tip (planar) and the other with the molecule bridging between two electrodes using carboxylic acids as anchoring groups (upright). The junctions with planar molecular orientation have a conductance that is significantly higher (by a factor of 400) than junctions with molecules in an upright geometry.

Conclusion.

Employing an electrochemical STM set up enables us to control the orientation of single molecules between two gold electrodes and, for the first time, measure the conductance in a controlled manner along two different axes. We developed a strategy to use the potential of the gold (working) electrode to controllably change the orientation of benzenecarboxylic acids in the junction from planar to upright and to measure the conductance of single molecules either perpendicular to or along the benzene ring. The measured conductance of TMA molecules in these two distinct orientations determined the two conductance states of the single molecule in the junction. Hence, we introduce a new class of single-molecule junctions that exhibit well-defined orientation-dependent anisotropic conductivity. Furthermore, the junctions with planar molecular orientation have a conductance significantly higher (by a factor of ~400) than junctions with molecules in an upright geometry. Thus, we can use the electrode potential as a knob to design a single molecule electromechanical switch with high on to off conductance ratios. We suggested this phenomenon is applicable in designing single molecule switches where the orientation of the molecules in the junctions is controlled utilizing the electrode potential as a knob. This offers a new method for designing a robust, room-temperature electromechanical single molecule switches with high "ON" to "OFF" conductance ratios.

Experimental Section

Electrochemical Scanning Tunneling Microscopy (EC-STM) Imaging: STM images were obtained with a PicoScan STM system (Molecular Imaging). The PicoStat bipotentiostat (Molecular Imaging) was used to control the surface and tip potential independently. Platinum wires were used as the quasi-reference electrode and the counter electrode. STM tips were prepared by electrochemically etching 0.25 mm diameter tungsten wires in 2 M NaOH solution using a platinum ring electrode. Tips, coated with polyethylene, yielded less than 10 pA Faradic current. All the STM images were obtained under constant current mode. Additional details of the STM experiment can be found in the caption of each image reported.

Electrochemical Scanning Tunneling Microscopy Break Junction (EC-STM-BJ): The Electrochemical STM break junction (EC-STM-BJ)

experiments were carried out with a Keysight Picoscan (Molecular Imaging) microscope under electrode potential control. 1 μ A/V and 10 nA/V pre-amplifiers were used for all SMC measurements. STM software drove the tip to approach the gold surface in the STM cell while the surface and the tip potentials were controlled using the PicoStat bipotentiostat. In STM break junction (STM-BJ) experiments, the STM tip is repeatedly brought into and out of contact with another electrode in the presence of molecules while current-distance traces are recorded. The displacement of the two electrodes (the STM tip and the substrate) without molecules bridging between them gives rise to quasi exponentially decaying traces. When a molecular junction forms, the current remains approximately constant even as the electrode-electrode distance increases so that a current plateau or step appears in the traces. The current drops exponentially with distance when the junction breaks. The histogram generated from the measured current-distance traces contains peaks that can be ascribed to charge transport through single molecules. Thus, the conductance of single molecules can be determined. For individual current-distance traces, the tip was driven into contact with the substrate to form a junction at a sweep rate of 16-26 nm/s. The tip was then retracted to break the contact. The process of the forming and breaking of junctions was repeated many times and a large number of current-distance traces were recorded for statistical analysis.

STM-BJ data analysis: To generate each histogram, more than 2000 individual current-distance traces were collected and analyzed without selection. Current-distance traces were collected only when the individual curves showed current saturation reflecting tip-surface contact, followed by sharp decay of current after pulling the tip away from the surface. As soon as the curves no longer showed current saturation at the tip-surface contact, we stopped recording data, repositioned the tip and resumed measurements. Data collection restarted when current saturation could be achieved for the tip-surface contact.

Acknowledgements

The authors acknowledge funding for this work from National Science Foundation (CHE-1508567) and as part of the Center for the Computational Design of Functional Layered Materials, an Energy Research Center funded by the U.S. Department of Energy, Office of Science, Basic Energy Sciences, under Grant No. DE-SC0012575.

Keywords: Molecular electronics • Molecular switch • Single molecule charge transport • Single molecule studies • STM Break junction

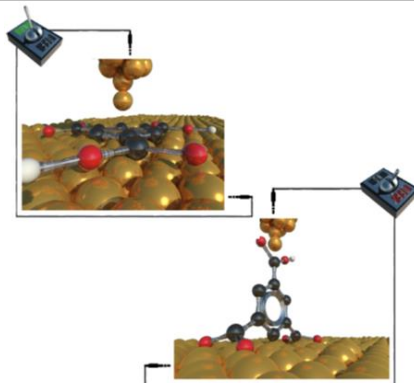
- [1] A. H. Flood, J. F. Stoddart, D. W. Steuerman, J. R. Heath, *Science* **2004**, *306*, 2055–2056.
- [2] A. Aviram, M. A. Ratner, *Chem. Phys. Lett.* **1974**, *29*, 277–283.
- [3] M. del Valle, R. Gutierrez, C. Tejedor, G. Cuniberti, *Nat. nanotechnol.* **2007**, *2*, 176–179.
- [4] B. Xu, N. J. Tao, *Science* **2003**, *301*, 1221–1223.
- [5] Z. Li, M. Smeu, M. A. Ratner, E. Borguet, *J. Phys. Chem. C* **2013**, *117*, 14890–14898.
- [6] X. Li, J. He, J. Hihath, B. Xu, S. M. Lindsay, N. Tao, *J. Am. Chem. Soc.* **2006**, *128*, 2135–2141.
- [7] F. Chen, X. Li, J. Hihath, Z. Huang, N. Tao, *J. Am. Chem. Soc.* **2006**, *128*, 15874–15881.
- [8] N. J. Tao, *Nat. Nanotechnol.* **2006**, *1*, 173–181.

- [9] A. Nitzan, M. A. Ratner, *Science* **2003**, *300*, 1384–1390.
- [10] S. Afsari, Z. Li, E. Borguet, *Angew. Chem. Int. Ed.* **2014**, *53*, 9771–9774.
- [11] Z. Li, H. Li, S. Chen, T. Froehlich, C. Yi, C. Schönenberger, M. Calame, S. Decurtins, S. X. Liu, E. Borguet, *J. Am. Chem. Soc.* **2014**, *136*, 8867–8870.
- [12] M. Mine, T. Tsutsui, E. Miyoshi, *Jpn. J. Appl. Phys.* **2008**, *47*, 8033–8038.
- [13] H. Wang, Z. Jiang, Y. Wang, S. Sanvito, S. Hou, *ChemPhysChem* **2016**, *17*, 2272–2277.
- [14] Y. Komoto, S. Fujii, T. Nishino, M. Kiguchi, *Beilstein J. Nanotechnol.* **2015**, *6*, 2431–2437.
- [15] M. Kiguchi, H. Nakamura, Y. Takahashi, T. Takahashi, T. Ohto, *J. Phys. Chem. C* **2010**, *114*, 22254–22261.
- [16] J. N. Ladenthin, T. Frederiksen, M. Persson, J. C. Sharp, S. Gawinkowski, J. Waluk, T. Kumagai, *Nat. Chem.* **2016**, *8*, 935–940.
- [17] C. Jia, A. Migliore, N. Xin, S. Huang, J. Wang, Q. Yang, S. Wang, H. Chen, D. Wang, B. Feng, et al., *Science* **2016**, *352*, 1443–1446.
- [18] B. E. Tebikachew, H. B. Li, A. Pirrotta, K. Börjesson, G. C. Solomon, J. Hihath, K. Moth-Poulsen, *J. Phys. Chem. C* **2017**, *121*, 7094–7100.
- [19] L. J. O'Driscoll, J. M. Hamill, I. Grace, B. W. Nielsen, E. Almutib, Y. Fu, W. Hong, C. J. Lambert, J. O. Jeppesen, *Chem. Sci.* **2017**, *8*, 6123–6130.
- [20] Z. Li, M. Smeu, S. Afsari, Y. Xing, M. A. Ratner, E. Borguet, *Angew. Chem. Int. Ed.* **2014**, *53*, 1098–1102.
- [21] C. D. Frisbie, *Science* **2016**, *352*, 1394–1395.
- [22] Z. Li, B. Han, L. J. Wan, T. Wandlowski, *Langmuir* **2005**, *21*, 6915–6928.
- [23] S. Wu, J. Lipkowski, O. M. Magnussen, B. M. Ocko, T. Wandlowski, *J. Electroanal. Chem.* **1998**, *446*, 67–77.
- [24] B. Han, Z. Li, S. Pronkin, T. Wandlowski, *Can. J. Chem.* **2004**, *82*, 1481–1494.
- [25] B. Han, Z. Li, T. Wandlowski, *Anal Bioanal Chem* **2007**, *388*, 121–129.
- [26] X. Xiao, B. Xu, N. Tao, *J. Am. Chem. Soc.* **2004**, *126*, 5370–5371.
- [27] M. A. Reed, *Science* **1997**, *278*, 252–254.
- [28] J. Ulrich, D. Esrail, W. Pontius, L. Venkataraman, D. Millar, L. H. Doerrer, *J. Phys. Chem. B* **2006**, *110*, 2462–2466.
- [29] M. Lackinger, S. Griesl, T. Markert, F. Jamitzky, W. M. Heckl, *J. Phys. Chem. B* **2004**, *108*, 13652–13655.
- [30] M. Soler, E. Artacho, J. D. Gale, A. Garc, J. Junquera, P. Ordej, S. Daniel, *J. Physics-Condensed Matter* **2002**, *11*, 2745.
- [31] N. Papior, N. Lorente, T. Frederiksen, A. Garcia, *Comput. Phys. Commun.* **2017**, *212*, 8–24.
- [32] N. Troullier, J. L. Martins, *Phys. Rev. B* **1991**, *43*, 8861–8869.
- [33] K. Berland, P. Hyldgaard, *Phys. Rev. B* **2014**, *035412*, 1–8.
- [34] H. Peng, Z. Yang, J. P. Perdew, J. Sun, *Phys. Rev. X* **2016**, *041005*, 1–15.

Entry for the Table of Contents

RESEARCH ARTICLE

Anisotropic conductivity enables an electromechanical single molecule switch that toggles between "ON" and "OFF" states reversibly by changing the electrode potential.



*Sepideh Afsari, Parisa Yasini, Haowei Peng, John P. Perdew, Eric Borguet**

Page No. – Page No.

Anisotropic conductivity at the single molecule scale